

NEAR FIELD DISTRIBUTION OF H- PLANE SECTORAL MULTI-LAYER SOLID DIELECTRIC HORNS AND SEPTUM POLARIZER

Alireza Bayat  
(Ph.D.)  
Imam Hossein University,  
Dept.of Electrical Eng.  
abaiaat @ ihu. ac. ir

Majid Sol eimanipour  
(Ph.D.)  
Imam Hossein University,  
De pt.of Electrical Eng.  
msoleimani @ ihu.ac.ir

Mitra Tourabipourbanadkook  
(M.Tech.)  
Ministry of TCI  
Chair @ ICMRSE.ir

ABSTRACT

In this paper, near field distribution of H-plane sectoral multi-layer solid dielectric horn antennas has been analyzed theoretically under some simplifying assumptions for TE to X modes. Solution of Helmholtz equation is obtained for TE to X modes using separation of variables technique by assuming the horn to be made of an equivalent homogeneous dielectric material of dielectric constant equal to the equivalent of three dielectrics of slightly differing dielectric constants. On applying the proper boundary conditions i.e. the continuity of the electric and magnetic fields at the interfaces each between a dielectric region and a free space, transcendental equations for the transverse components of propagation constants are obtained. These transcendental equations are solved for the transverse propagation constants, for the fundamental mode and for two higher order modes for the horn of axial length = 6.34 cm and flare angle equal to 43.32°, and for the fundamental mode and for three higher order modes for the horn of axial length = 8 cm and flare angle = 43.32° at 10.2 GHZ. The theoretical aperture distributions obtained for these antennas are compared with corresponding experimental ones.

1.Introduction

Dielectric rod and horn antennas can compete well with small horns for some applications [1]. It has been shown that dielectric horns are more directive than their metal counterparts [2]. When optimized, they may become an alternative to the present metallic feeders on reflector and lens antennas. Sectoral solid and hollow dielectric horn antennas have been studied by many investigators [1-4]. In this paper, the near field analysis of H-plane sectoral multi-layer solid dielectric horn has been carried out. Analysis of the field distribution of this type of antenna is complicated due to complex nature of the boundary and hence the present theoretical approach is based on some simplifying assumptions. The field components for TE to X modes for the multi-layer antenna have been obtained by solving the Helmholtz equation for an equivalent homogeneous solid dielectric horn using the separation of variables technique and applying the appropriate boundary conditions. The theoretical near field distributions for the antennas of axial lengths = 6.34 cm and 8 cm and flare angle =43.32° in each, are compared with the corresponding experimental at 10.2 GHZ in X-band.

2.Theoretical Analysis

A sketch of the H-plane sectoral multi-layer solid dielectric horn is shown on figure 1. The antenna is symmetrical about the mid plane. The analysis of the near field distribution for this type antenna is complicated due to the complex nature of the boundary. The analysis can be made simpler by reducing the existing boundaries by calculating the equivalent relative dielectric constant  $\epsilon_{eff}$  for the three dielectric layers on one side of the mid-plane of the antenna under the assumption of same electric field strength in the three layers. An equivalent homogeneous dielectrics horn and the coordinate system used to derive field components are shown in figure 2.  $\epsilon_{eff}$  may be written as [5].

$$\epsilon_{eff} = \frac{(V_1 \epsilon_1 + V_2 \epsilon_2 + V_3 \epsilon_3)}{(V_1 + V_2 + V_3)}$$

Where  $\epsilon_1, \epsilon_2$  and are the relative dielectric constants of the three layers and  $v_1, v_2, v_3$  are the volumes occupied by the respective layers as shown in figure 1. In terms of dielectric layers dimensions.

$$\epsilon_{eff} = \frac{[\frac{a}{2}Lb]\epsilon_1 + [L\frac{L \tan \theta}{2} - b]\epsilon_2 + \{ [L\frac{L \tan \theta}{2} - b]\} \epsilon_3}{[\frac{a}{2}Lb] + [\frac{L \tan \alpha}{2} - b]}$$

Where “a” and “b” are the broad- and narrow- dimensions of the throat of the antenna and “L” is the axial length from the throat.

Here TE to x-mode has been chosen for the analysis. Since axial components of both electric-and magnetic- fields,  $E_z$  &  $H_z$ , exist in this mode, the mode is called hybrid mode. The wave propagation is assumed to be along the z-direction with an  $\exp\{-j(\beta_z Z - \omega t)\}$  where  $\beta_z$  is the axial propagation constant and  $\omega$  is the angular frequency dependence.

The field components for TE to X mode are given by Harrington [6]:

$$\begin{aligned} E_x = 0 \quad ; \quad H_x &= \frac{1}{j\omega\mu} \left( \frac{\partial^2 \psi}{\partial x^2} + k^2 \right) \psi \\ E_y &= -\frac{\partial \psi}{\partial z} \quad ; \quad H_y = \frac{1}{j\omega\mu} \left( \frac{\partial^2 \psi}{\partial x \partial y} \right) \\ E_z &= \frac{\partial \psi}{\partial y} \quad ; \quad H_z = \frac{1}{j\omega\mu} \left( \frac{\partial^2 \psi}{\partial x \partial y} \right) \end{aligned} \quad (1)$$

Where  $\psi$  (called the potential function) is the solution of the Helmholtz equation  $[\nabla^2 + k^2]\psi = 0$ ,  $k = \omega\sqrt{\epsilon\mu}$ , is the angular frequency, and  $\epsilon$  and  $\mu$  represent the permittivity and permeability of the medium in question respectively. From the boundary condition requirements, the proper forms of the potential function  $\psi$  in different regions depicted in figure 2. Can be written as [4,7]:

$$\psi = \begin{cases} M_1 \cos(k_{xv} X) \cos(k_y Y) & v = 0 \\ M_2 \exp(-jk_{xv} X) \cos(k_y Y) & v = 1 \\ M_2 \exp(+jk_{xv} X) \cos(k_y Y) & v = 2 \\ M_2 \cos(k_{xv} X) \exp(-jk_{yv} Y) & v = 3 \\ M_2 \cos(k_{xv} X) \exp(+jk_{yv} Y) & v = 4 \\ M_2 \cos(k_{xv} X) \exp(jk_{yv} Y) & v = 5 \end{cases} \quad (2)$$

Where  $v = 1, 2, 3, 4, 5$  refers to a particular region (region “1” is a dielectric medium of relative dielectric constant =  $\epsilon_{eff}$ , and region “2”, “3”, “4”, & “5” are air).  $K_{xv}$  and  $K_{yv}$  are the transverse propagation constants in  $v^{th}$  region. The factor  $\exp\{-j(\beta_z Z - \omega t)\}$  is omitted from these expressions. The dependence of the potential function on region “1” has been assumed co-sinusoidal on both x-and y-directions. It is well known that the field outside a dielectric rod decays exponentially. Therefore in regions “2” and “3”, the potential functions are assumed to vary co-sinusoidally along Y, and exponentially along X, those in region “4” and “5” vary co- sinusoidally along X and exponentially along Y in the same way as if the equivalent solid dielectric horn had been an uniform rectangular dielectric slab [8].

To match the fields at the boundaries between region “1” and regions “2” & “3”, it is assumed that.

$$K_{y1} = K_{y2} = K_{y3} = K_y \quad (3)$$

$$K_{x2} = K_{x3}$$

Similarly to match the fields between the regions “1” and regions “4” & “5”, it is assumed that

$$K_{x1} = K_{x4} = K_{x5} = K_x \quad (4)$$

$$K_{y4} = K_{y5}$$

The propagation constant  $K_{xy}$ ,  $K_{yv}$  and  $\beta_z$  are relate by the equation

$$K_{xy}^2 + K_{yv}^2 + \beta_z^2 = K_z^2 \quad (5)$$

#### Boundary Conditions

Tangential components of electric and magnetic fields at the boundaries are continuous, i.e.

$$E_{y1} = E_{y2} \Big|_{x = \left(\frac{a}{2} + z \tan \alpha\right)} \quad (6a)$$

$$E_{x1} \cos \alpha + E_{x1} \sin \alpha = E_{x2} \cos \alpha + E_{x2} \sin \alpha \Big|_{x = \left(\frac{a}{2} + z \tan \alpha\right)} \quad (8a)$$

$$E_{x1} = E_{x4} \Big|_{y = \frac{b}{2}} \quad (10a)$$

$$E_{x1} = E_{x5} \Big|_{y = -\frac{b}{2}} \quad (10b)$$

$$E_{y1} = E_{y3} \Big|_{x = \left(\frac{a}{2} + z \tan \alpha\right)} \quad (6b)$$

$$E_{x1} \cos \alpha - E_{x1} \sin \alpha = E_{x3} \cos \alpha - E_{x3} \sin \alpha \Big|_{x = \left(\frac{a}{2} + z \tan \alpha\right)} \quad (8b)$$

$$H_{x1} = H_{x4} \Big|_{y = \frac{b}{2}} \quad (11a)$$

$$H_{x1} = H_{x5} \Big|_{y = -\frac{b}{2}} \quad (11b)$$

$$H_{y1} = H_{y2} \Big|_{x = \left(\frac{a}{2} + z \tan \alpha\right)} \quad (7a)$$

$$H_{z1} \cos \alpha + H_{z1} \sin \alpha = H_{z2} \cos \alpha + H_{z2} \sin \alpha \Big|_{x = \left(\frac{a}{2} + z \tan \alpha\right)} \quad (9a)$$

$$H_{x1} = H_{x4} \Big|_{y = \frac{b}{2}} \quad (12a)$$

$$H_{x1} = H_{x5} \Big|_{y = -\frac{b}{2}} \quad (12b)$$

$$H_{y1} = H_{y3} \Big|_{x = \left(\frac{a}{2} + z \tan \alpha\right)} \quad (7b)$$

$$H_{z1} \cos \alpha - H_{z1} \sin \alpha = H_{z3} \cos \alpha - H_{z3} \sin \alpha \Big|_{x = \left(\frac{a}{2} + z \tan \alpha\right)} \quad (9b)$$

Where “a” is the broad cross-sectional dimension of the feeder (2.286 cm), “b” is the narrow dimension of the feeder (=1.016cm), z=“L” is the axial length of the horn, and “α” is the half-flare angle. The potential functions (equation (2)) are substituted in to equation (1) for various field components. The resulting field expressions are substituted in to boundary conditions (equations (6) to (12)) and use is made of equations (3), (4), and (5) to obtain transcendental equations for transverse propagation constants  $K_x$  and  $K_y$ , which can be written as:

$$K_x \tan \left\{ K_x \left( \frac{a}{2} + z \tan \alpha \right) \right\} = (K_1^2 - K_0^2 - K_x^2)^{1/2} \quad (13)$$

$$K_y \tan \left( K_y \frac{b}{2} \right) = (K_1^2 - K_0^2 - K_y^2)^{1/2}$$

In the derivation of the transcendental equations it is assumed that

$$\mu_1 = \mu_2 = \mu_3 = \mu_4 = \mu_5 = \mu_0 \quad \& \quad K_1^2 = \epsilon_{eff} K_0^2 \quad (14)$$

$$K_2 = K_3 = K_4 = K_5 = K_0 = -\omega (\mu_0 \epsilon_0)^{1/2}$$

Since the equivalent dielectric constant of the horn is non-magnetic and the regions 2, 3, 4, & 5 are the same (air), and  $\epsilon_0$  are the permittivity and permeability of the air regions and  $\epsilon_{eff}$  is the effective value of relative dielectric constant of the equivalent homogeneous solid dielectric horn.

The values of transverse propagation constants  $K_x$  and  $K_y$  for the fundamental and higher order modes were computed for the horns of axial lengths = 6.34 and 8 cm and flare angle = 43.32° in each case at 10.2 GHz. The dimensions of these multi-layer horns (figure 1.) are given below:

Axial Length (L) cm	Flare Angle (2)(Degree)	“a” (cm)	“b” (cm)	“ED” (cm)	“DC” (cm)	
Horn 1	6.34	43.32	2.286	1.016	2.221	0.391
Horn 2	8.00	43.32	2.286	1.016	2.762	0.415

Once the values of transverse propagation constants for these antennas are found out, values of axial propagation constant can be calculated.

The near field expression for TE to x-modes is given by the following formula

$$E_y = M_1 j \beta_z \cos(K_x X) \cos(K_y Y) \exp\{j(\omega t - \beta_z Z)\} \quad (15)$$

Putting the values of transverse- and axial- propagation constants for different modes in the expression for the relative field strength at different points across the aperture of the horn were computed. The theoretical near field distributions for different modes for the multi-layer horn of axial length 6.34 cm and flare angle = 43.32° length = 8 cm and flare angle = 43.32° are given in figure 4.

#### 4. Experiments and Results

The measurement of near field amplitudes across the aperture of the two H-plane sectoral multi-layer solid dielectric horns of axial lengths = 6.34 and 8 cm and flare angle = 43.32° in each case is carried out at 10.2 GHz. The experimental set-up is shown in figure 5. Microwave source is a Gunn oscillator from which microwave signal of frequency = 10.2 GHz is generated and modulated with 1 KHZ square wave. The modulated microwave signal is fed, through other necessary components (isolator, variable attenuator, frequency meter, 20 dB directional coupler, and E-H tuner) to the antenna under test. The probe used to sample power across the aperture of the antenna under test is an extended central conductor of rigid co-axial cable. E-H. tuner is used to maximise the power fed to the antenna. 20dB directional coupler is used to sample the power fed to the antenna. Square law crystal detector is used to detect the microwave power picked-up by the probe.

Following this procedure, the near field distributions of the two antennas are measured. Experimental near field distributions are plotted in figures 3 & 4 respectively for the two antennas of axial lengths = 6.34 and 8 cm and flare angle = 43.32° in each.

It can be seen from figures 3 & 4 that theoretical distributions for the fundamental mode for these antennas are not in very good agreement with corresponding experimental distributions.

Fig6. shows simulated and measured return loss curves. The measurements were affected by WR-90 standard X-band adaptor specifications, but finally the measured VSER value was less than 1.15, that is acceptable for the requirements.

## Septum polarizer

This contribution presents new design dimensions for the ridge waveguide septum polarizer. Emphasis is placed first on including the finite septum thickness in the analysis; second, demonstrating third, including a stepped approach for extremely thin septa, fourth, optimizing components without the need for additional phase – adjusting structures, add fifth, providing the application engineers with sound design guidelines.

Stepped septum in a square waveguide is a very interesting device to excite high purity left – hand or right hand circular polarization in a circular waveguide [9]. It uses an extremely compact element which handles the tasks of both the orthomode transducers (OMT) and polarizer.

## A. Theory

The stepped septum polarizer in square waveguide technology is well known for its application as orthomode transducer. This object consists of a square waveguide and a metal stepped plate (septum). The field transition inside the septum polarizer is shown in fig 7. A field component (in the square waveguide) perpendicular to the septum transforms into two even –mode signals in the rectangular ports; parallel components transform into two odd-mode signals. If both components exist simultaneously, cancellation can occur in one rectangular port, provided the amplitudes are identical and phases are correct. For example if a RHCP field is propagating toward the septum its two orthogonal components will be as shown in fig 8 with the vertical component leading the horizontal by 90°. The septum region is equivalent to a single –rigid waveguide to the vertical component, and it is delayed in phase relative to the horizontal one. A properly designed septum allows obtaining a differential delay equal to 90°, resulting in field cancellation in port L and reinforcement in port R.

## B. Design

Based on our knowledge, four sections constant thickness septum polarizer has a good performance for our desired design. The input square waveguide has the dimensions of  $a=b=22.86$ , that is divided by a septum with thickness  $t=2.54$  mm, provide two output ports of standard X-band waveguide ( $0.9 \times 0.4$ ). Each port was connected to 90° waveguide bend to separate the ports mechanically and provide ability to connect to standard WR-90 waveguide connector. The septum steps, length and heights, were designed and optimized to have input return loss better than  $-30$  dB, 30 dB port to port isolation, and less than 0.5 dB axial ratio on the operating 8-8.4 GHz frequency band. All the simulations have been performed with HFSS code and there were very good agreement between simulation and laboratory measurements. The total length of the constructed stepped septum polarizer by constructed stepped septum polarizer by considering the 90° bend was 120 mm.

## 5. conclusions

In this paper, attempts have been made to find the near field analysis for H-plane sectoral multi-layer solid dielectric horn under several simplifying assumptions and to compare the theoretical near field distributions with the experimental ones. The theoretical near field distributions for the fundamental mode for these antennas are not in very good agreement with the corresponding experiment distributions. The reasons for disagreement may be due to:

- (I) the generation of unaccounted higher order modes ,
- (II) surface wave assumption not being fully valid,
- (III) approximation made in arriving at the effective relative dielectric constant value not being fully valid,
- (IV) reflections occurring at each interface between two dielectrics of the multi-layer horn

An appropriate septum polarizer was designed and constructed to receive the desired circular polarized signal without needing any hybrid circuits or orthomode transducer (OMT). To match the feed input (cylindrical waveguide) and septum polarizer (square waveguide) an appropriate circular to square transmission was designed and used in the final system application.

A very good agreement between simulations and measurements has been obtained.

This system could be used for special low bandwidth and dual-circular polarized satellite data link. New profiled corrugated horns and reflector systems are under development.

## Reference

- [1] J.R. James, “Engineering Approach to the Design of Tapered dielectric Rod & Horn Antennas”, Radio Electron, Engg., vol. 42 , pp. 251-259, June 1972.
- [2] R.K. Jha, D.K. Mishra, and L. Jha, “A Comparative study of Dielectric and Metallic Horn Antennas”, IEEE-IERE India, Feb. 1975.
- [3] R.K. Jha and A.Aas, “H-Plane Sectoral Dielectric Horn Antennas”, IEEE-IERE Proc. India, No.2, pp. 69-77, March-April 1997.
- [4] A.K. Singh, B. Jha, and R.K. Jha, “Near Field Analysis of H-Plane Hollow Sectoral Dielectric Horn Antennas”, International Journal of Electronic, Vol. 68, No.6, pp. 1055-1061, 1990.
- [5] L.N. Loshakov and E.B. OL “dergge” “Propagation of slow waves along a Helix with Dielectric Support”, Radio Engineering & Electronic Physics, Vol. 13, No.1, pp. 45-51, 1968.
- [6] R.F. Harrington, Time Harmonic Electromagnetic fields, Mc Grow Hill Book co. , New York 1961.
- [7] E.A.C. Marcatilli, “Dielectric Rectangular Waveguide and Directional Coupler for Integrated Air Unit”, BSTJ, Vol. 48, No.7, pp. 2071-2102, 1969.
- [8] P.J.B. Clarricoats and C.E.R.C. Salema, “Antennas Employing Conical Dielectric Horns Part I & II”, Proc. IEE, Vol. 120, pp. 741-749; 750-756, July, 1973.
- [9] Behe, R; Brachat, P, “compact duplexer- polarizer with semicircular waveguide” IEEE transaction on Antennas and propagation, vol. 39 Issue: 8 Aug 1991.

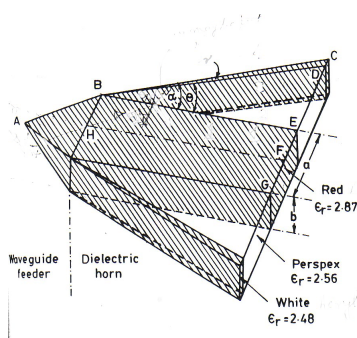


Fig 1. H-plane sectoral multilayer solid dielectric horn

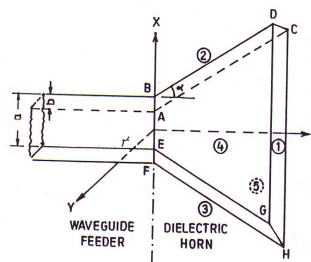


Fig 2. CO-Ordinate system of H-plane sectoral equivalent solid dielectric horn.

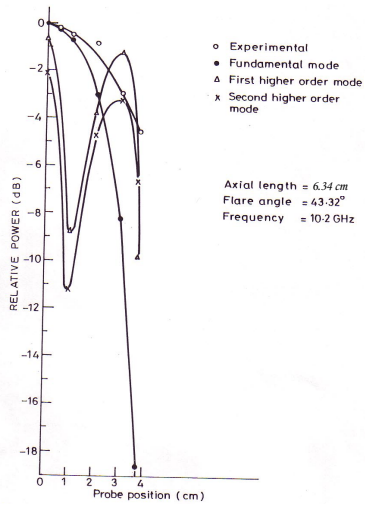


Fig 3. Near field Distributions of H- plane sectoral Multi-layer solid dielectric horn of axial length = 6.34 cm and flare angle =43.32°

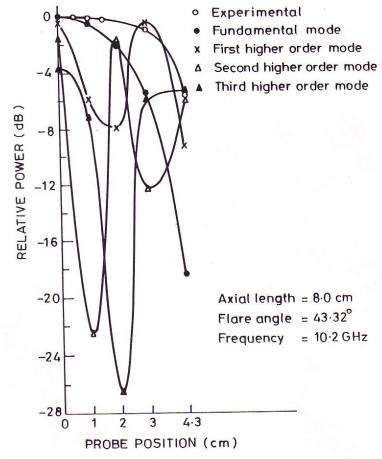


Fig 4. near field distributions of H-plane sectoral multi-layer solid dielectric horn of axial length =8cm and flare angle =43.32°.

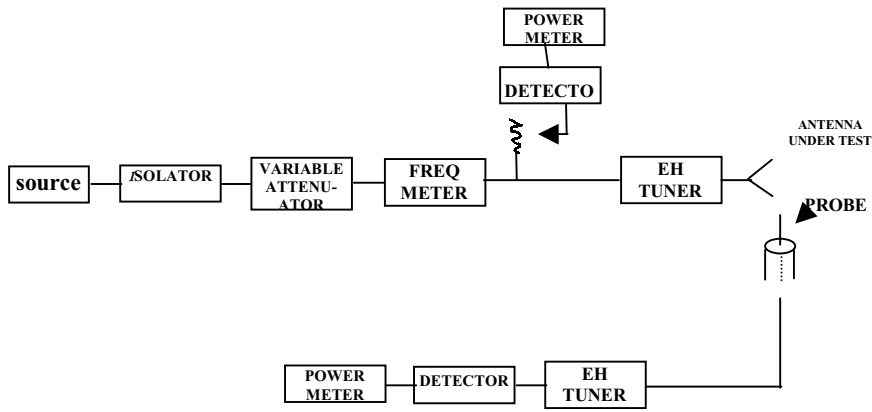


Fig 5. Experimental set-up for measuring the near field distribution

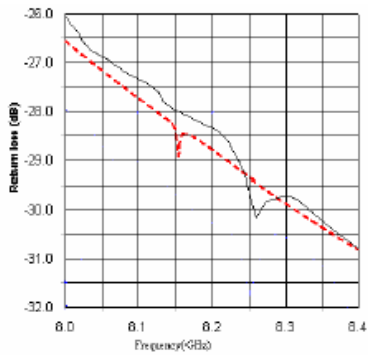


Fig 6. simulated and measured return loss

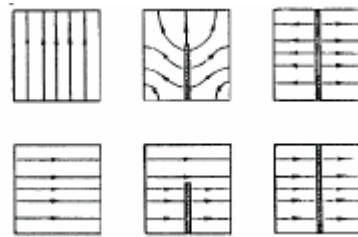


Fig 7. field transition inside the square waveguide

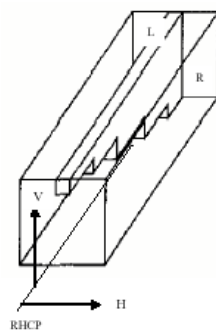


Fig 8. polarizer operation